Quaternary Research 71 (2009) 108–120

Contents lists available at ScienceDirect

Quaternary Research

journal homepage: www.elsevier.com/locate/yqres

The Iberian–Roman Humid Period (2600–1600 cal yr BP) in the Zoñar Lake varve record (Andalucía, southern Spain)

Celia Martín-Puertas [a,*], Blas L. Valero-Garcés [b], Achim Brauer [c], M. Pilar Mata [a], Antonio Delgado-Huertas [d], Peter Dulski [c]

[a] Departamento de Ciencias de la Tierra-CASEM, University of Cádiz. Avd. Saharaui s/n Puerto Real E-11510 Cádiz, Spain
[b] Instituto Pirenaico de Ecología-CSIC, Apdo 202, E-50080 Zaragoza, Spain
[c] GeoForschungsZentrum Potsdam, Section 3.3, Climate Dynamics and Sediments, Telegrafenberg, D-14473 Potsdam, Germany
[d] Departamento de Ciencias de la Tierra y Química Ambiental, Estación Experimental del Zaidín-CSIC, E-18008 Granada, Spain

ARTICLE INFO

Article history:
Received 31 March 2008
Available online 18 December 2008

Keywords:
Holocene
Mediterranean region
Lake varve chronology
Spain
Solar variability
Iberian–Roman period

ABSTRACT

The Iberian–Roman Humid Period (IRHP, 2600–1600 cal yr BP), is the most humid phase of the last 4000 yr in southern Spain as recorded in the sedimentary sequence of Zoñar Lake (37°29′00″N, 4°41′22″ W, 300 m a.s.l.). A varve chronology supported by several AMS ^{14}C dates allows study of the lake evolution at annual scale in response to human impact and climate changes. There are four climate phases within this period: i) gradual transition (2600–2500 yr ago, 650–550 BC) from a previous arid period; ii) the most humid interval during the Iberian–Early Roman Epoch (2500–2140 yr ago, 550–190 BC); iii) an arid interval during the Roman Empire Epoch (2140–1800 yr ago, 190 BC AD 150); and iv) a humid period synchronous with the decline of the Roman Empire (1800–1600 yr ago, AD 150–350). Varve thickness and geochemical proxies show a multi-decadal cyclicity similar to modern North Atlantic Oscillation (NAO) (60, 20 years) and solar variability cycles (11 yr). The timing and the structure of this humid period is similar to that described in Eastern Mediterranean and northern European sites and supports the same large-scale climate control for northern latitudes and the Mediterranean region.

Introduction

The annual nature of some laminated sediments (varves) provides a useful tool for high resolution reconstruction of climate and environmental changes based on varve thickness, internal structure variations and a number of sedimentological, geochemical and biological proxies. The strong seasonality of the Mediterranean climate, the relatively deep, meromictic nature of some karstic lakes and the occurrence of algal blooms in spring time are conducive to the genesis and preservation of varved sediments in some lakes in the Iberian Peninsula (Juliá et al., 1998; Rodrigo et al., 2001). The sedimentary record from Zoñar Lake (Andalusia, southern Spain) spans the last 4000 years (Martín-Puertas et al., 2008), and the 2600–1600 cal yr BP period is represented by finely laminated, varved sediments.

In this paper we focus on the varved section of the Zoñar record (2600 to 1600 cal yr BP) that reflects humid conditions in the area. Several studies have shown that dry conditions dominated the Mediterranean region from 4000 to 2800 cal yr BP (Heim et al., 1997; Issar, 2003), followed by a shift to a wetter and cooler climate in Europe (Van Geel et al., 1996) and wetter conditions in the Mediterranean area (Roberts et al., 2004; Luterbacher et al., 2006; Zanchetta et al., 2007). Moreover, archaeological data and historical documents provide some evidences of moister conditions in the Mediterranean region during the Roman Classical Period and comparatively drier conditions from 2000 years ago to present (Reale and Dirmeyer, 2000). However, other records, as Lake Frassino (Baroni et al., 2006), suggest a drier late Holocene in the Mediterranean area. Such discrepancies may reflect processes linked to changes in seasonality or regional variability between Mediterranean sites (Magny et al., 2007). The Zoñar varved record provides the opportunity to study the seasonality of the Mediterranean climate during a wetter period controlled by similar climate patterns as nowadays and to evaluate the interactions of past societies with climate fluctuations in southern Spain.

Study area

Zoñar Lake (37°29′00″N, 4°41′22″ W, 300 m a.s.l.) is the deepest (14. 5 m) and largest lake (37 ha, surface area) (Valero-Garcés et al., 2006), in the Guadalquivir River Basin (southern Spain). The origin of this small lake basin has been related to karstic activity along some fault structures (Sánchez et al., 1992). The lake has no surface functional outlet and the inlets are temporary. The inputs during an average year are rainfall (0.177 Hm^3), runoff (0.168 Hm^3), groundwater (0.4 Hm^3) and springs (Escobar, Zoñar and Eucaliptus, Fig. 1a)

* Corresponding author. Fax: +34 956016195.
E-mail address: celia.martin@uca.es (C. Martín-Puertas).

0033-5894/$ – see front matter © 2008 University of Washington. All rights reserved.
doi:10.1016/j.yqres.2008.10.004

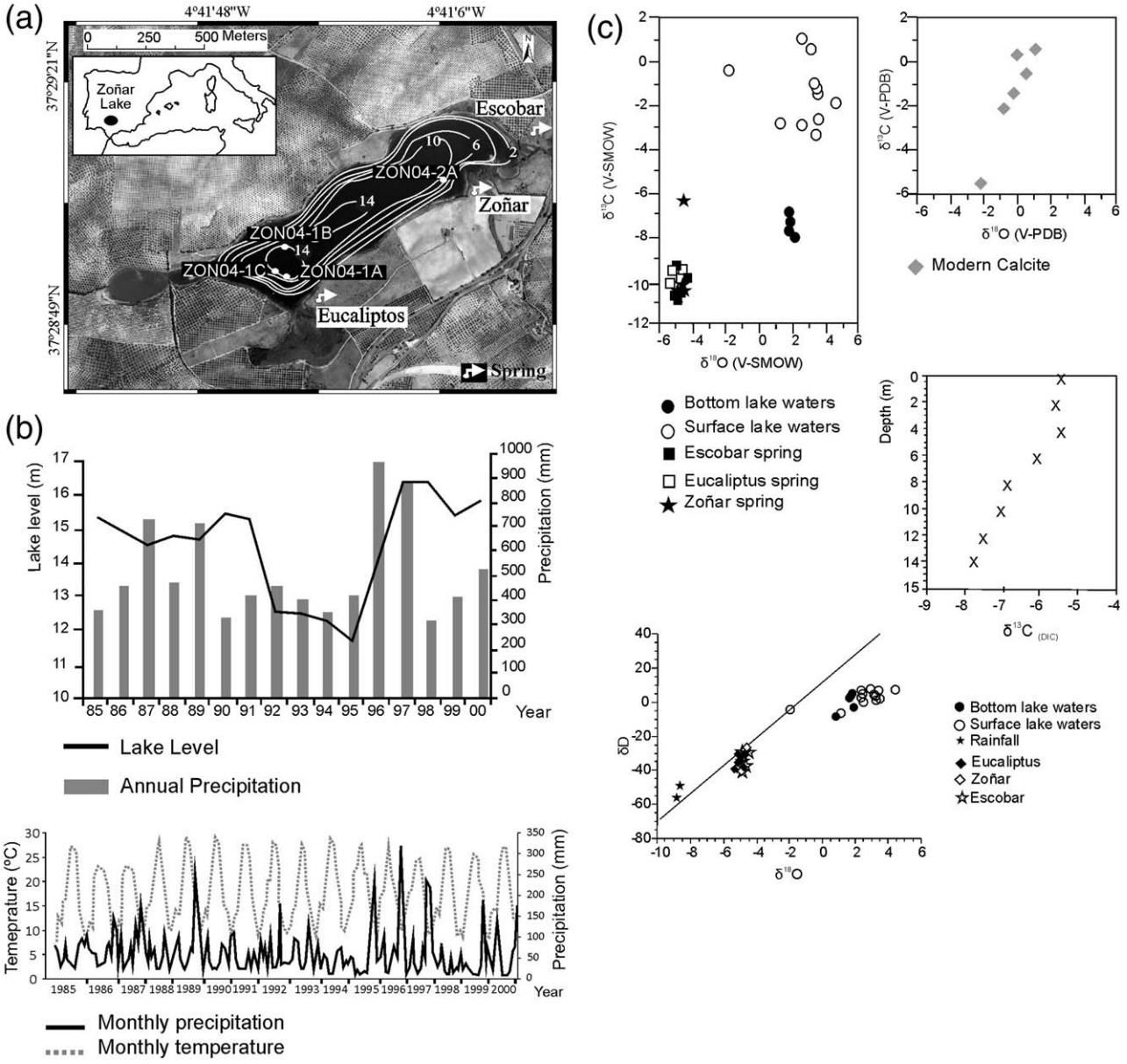

Figure 1. (a) Zoñar Lake location in the Mediterranean area. The Zoñar Lake catchment and a bathymetric map over the aerial photograph. (b) Annual precipitation and maximum lake level from 1985 to 2000. Monthly precipitation and temperature average from 1985 to 2000. (c) 1. Stable oxygen and carbon isotopic composition of lake and spring waters and modern calcite precipitated in the lake. 2. Oxygen and deuterium isotope composition of lake waters, springs and rainfall 3. A $\delta^{13}C$ depth profile showing water stratification and heavy isotope enrichment in epilimnetic waters.

(0.073 Hm^3); and the main output is evaporation (0.8 Hm^3) (Enadimsa, 1989; Moya, 1986). The lake waters are saline (2. 4 g/l) and the lake is monomictic, with a thermocline at 4 m depth in summer and a mixed period in winter. Spring waters are of (HCO_3^-)–(Ca^{2+}) type, while the lake waters are of (Cl^-)–(Na^+) type. A hydrological survey during the years 1984–1985 (Moya, 1986) and the data collected by the regional government since 1982, show that both lake level and spring flows quickly respond to rainfall (Fig. 1b) and that during the prolonged dry period of 1992–1995, lake level dropped to a minimum of 11 m.

Water stratification is also shown by isotopic compositions, with surface waters more enriched in ^{18}O (about 1 to 2‰) and ^{13}C (between 4 and 9‰) than bottom waters (Fig. 1c), reflecting preferential photosynthetic uptake of ^{12}C in the epilimnion and decomposition of organic matter in the hypolimnion (Myrbo and Shapley, 2006). All the spring waters have similar isotopic compositions (δD between −30 and −40‰ and δ ^{18}O around −5‰), slightly more evolved than rainfall precipitation (−50 and −9‰, respectively) but still plotting along the global meteoric water line (Fig. 1c). The lake waters have higher isotopic values, indicative of significant evaporative processes affecting the lake.

The area has a semi-humid Mediterranean climate (Valero-Garcés et al., 2006; Martín-Puertas et al., 2008). Meteorological data from 1985 to 2000 show seasonality pattern change, where the most precipitation occurs during the winter or spring (Fig. 1b), leading to weaker water stratification in the lake.

Methods

Four sediment cores were collected with a Kullenberg piston corer from the deepest part of the lake (14–15 m) in 2004. Varved sediments, corresponding with the Iberian–Roman Humid Period

(IRHP) (Martín-Puertas et al., 2008) occurred in all cores. The varved interval was sampled in two cores (ZON04-1B-1K; ZON04-1C-1K) (136 cm from core 1B and 130 cm from core 1C) for thin sections and a composite profile for the laminated interval was compiled. Thin sections (100×15×35 mm) were prepared using the freeze-dry technique (liquid nitrogen) and subsequent impregnation with epoxy resin (araldite) under vacuum (Brauer and Casanova, 2001). Optical microscope analyses were used to study the microfacies and to count the varves. The varve thickness measurement were carried out on three continuous series of overlapping (2 cm) thin sections in cores 1B and 1C for the same interval. Three ^{14}C AMS dates were obtained from plant remains (seed, terrestrial plant and olive pit) in the laminated interval.

An X-Ray Fluorescence (XRF) core scanner was used to measure Al, Si, P, S K, Ca, Ti, Mn and Fe intensities (total counts) on core 1B (338–480 cm) with 2 mm resolution. The measurements were produced using 30 s count time, 10 kV X-ray voltage and X-ray current of 1 mA. For better resolution, Micro-XRF was applied to impregnated blocks of cores 1B (399–417 cm; 444–453 cm) and 1C (346–364 cm; 372–382 cm). The blocks were measured with 54 µm resolution for Mg, Al, Si, P, S, Cl, K, Ca, Ti, Mn, Fe and Sr elements (30 s count time, 40 kV X-ray voltage and 300 µA X-ray current). The data obtained by the micro-XRF core scanner are expressed as element intensities in counts per second (cps). Five calcite layers, three organic layers and four detrital layers were measured by micro-X-ray Difractometer (micro-XRD), and SEM studies were performed to characterize the different microfacies. A total of 87 calcite layers from the varves were sampled for ^{18}O and ^{13}C isotopic compositions on core 1B in the interval where lamination is best preserved (339–449 cm) to avoid allochthonous carbonate contamination. Isotope analyses were performed using standard techniques (McCrea 1950) using an IRMS Finnigan MAT 251. Spectral analysis of single time series of environmental indicators was performed by SPECTRUM based on the Lomb–Scargle Fourier transform for unevenly spaced data in combination with the Welch-Overlapped-Segment-Averaging procedure (Schulz and Stattegger, 1997).

Results

Chronology

The previous Zoñar age-depth model for the IRHP (Martín-Puertas et al., 2008) has been improved using a floating chronology based on varve counting linked to calendar time by radiocarbon dates. Three ^{14}C AMS dates, calibrated with CALIB 5.1 software and the INTCAL04 curve (Reimer et al., 2004) – 1865±30 ^{14}C yr BP (1722–1873 cal yr BP), 2165 ±30 ^{14}C yr BP (2097–2210 cal yr BP) and 2525±30 ^{14}C yr BP (2490–2643 cal yr BP) – were used as chronomarkers to establish an age-depth model (Fig. 2). A total duration of 637 yr resulted from 441 varve counts and thickness measurements, and 196 additional interpolated varves calculated from average sedimentation rates (1 varve/mm; Fig. 2) on some intervals with poor varve preservation. Possible errors occurring within varve chronology, attributed to sediment accumulation rates variations, have been considered within the calibrated error bars of radiocarbon data (Fig. 2).

The Iberian–Roman Humid Period occurred from 2600 to 1600 cal yr BP and included a 340 yr non-varved, gypsum-rich period between 1800 and 2140 cal yr BP (Fig. 2). Continuous varve formation and good preservation started at 455 cm sediment depth, (23 cm above the 2565±75 cal yr BP date), and lasted till 395 cm (2140 cal yr BP) showing favorable condition for varve preservation for about 400 varve years. After deposition of a massive layer at 1795±75 cal yr BP, a second varve stage started at 363 cm sediment depth and continued during 180 varves.

The Iberian–Roman period

Sedimentary microfacies

The IRHP is represented by a 142 cm long interval (338–480 cm sediment depth in core ZON04-1B) composed of the best finely laminated facies of the whole 6 m long Zoñar record. This interval is characterized by a sharp increase in *Olea* pollen percentages and a dominance of pelagic diatoms (Martín-Puertas et al., 2008) (Fig. 3). The compositional and textural features of the microfacies and the good coherence between the ^{14}C AMS time interval (from 2565 to 2155 cal yr BP, i.e. 410 yr) and the number of laminae within that interval (427), underlines the annual nature of the lamination (varves) (Fig. 2). The Zoñar varves are composed of three sub-layer types (Fig. 4a): i) a white *calcite layer* composed almost only by rhomboedric calcite crystals, 5–15 µm long (Fig. 4b) and containing abundant colonies of *Botryococcus braunii* Kutzing, 1849 (in Komárek and Marvan, 1992) (Figs. 4d, e). Optical microscopy and SEM observations show well preserved colonies of *Botryococcus* at the base and within the calcite layer (Figs. 4a, d, e). *B. braunii* colonies (Fig. 4e) are well preserved in sediments because their outer cell walls are resistant to physicochemical and biological degradation (Audino et al., 2001, and reference therein). The calcite layer is interpreted as endogenic precipitation of calcite in the epilimnion associated with ion saturation enhanced by algal blooms (Brauer, 2004); ii) a greenish *organic matter layer* composed of amorphous aquatic organic matter,

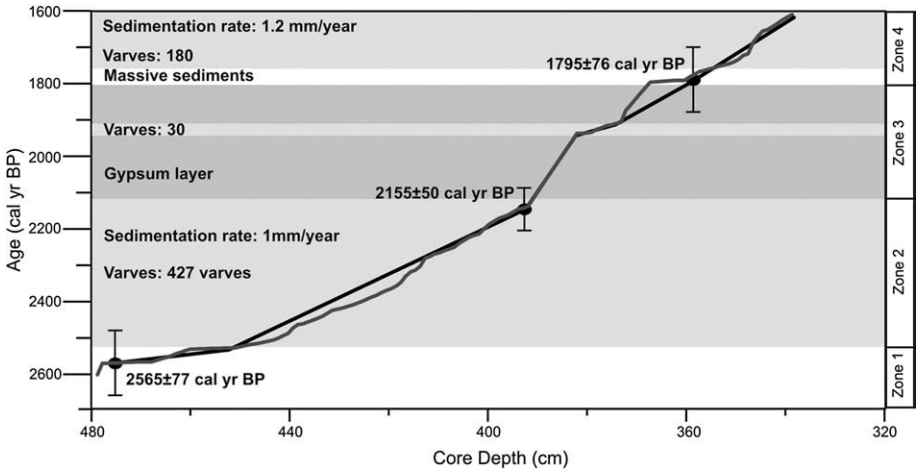

Figure 2. Age-depth model for the IRHP period in Zoñar Lake based on varve counting and AMS ^{14}C dates.

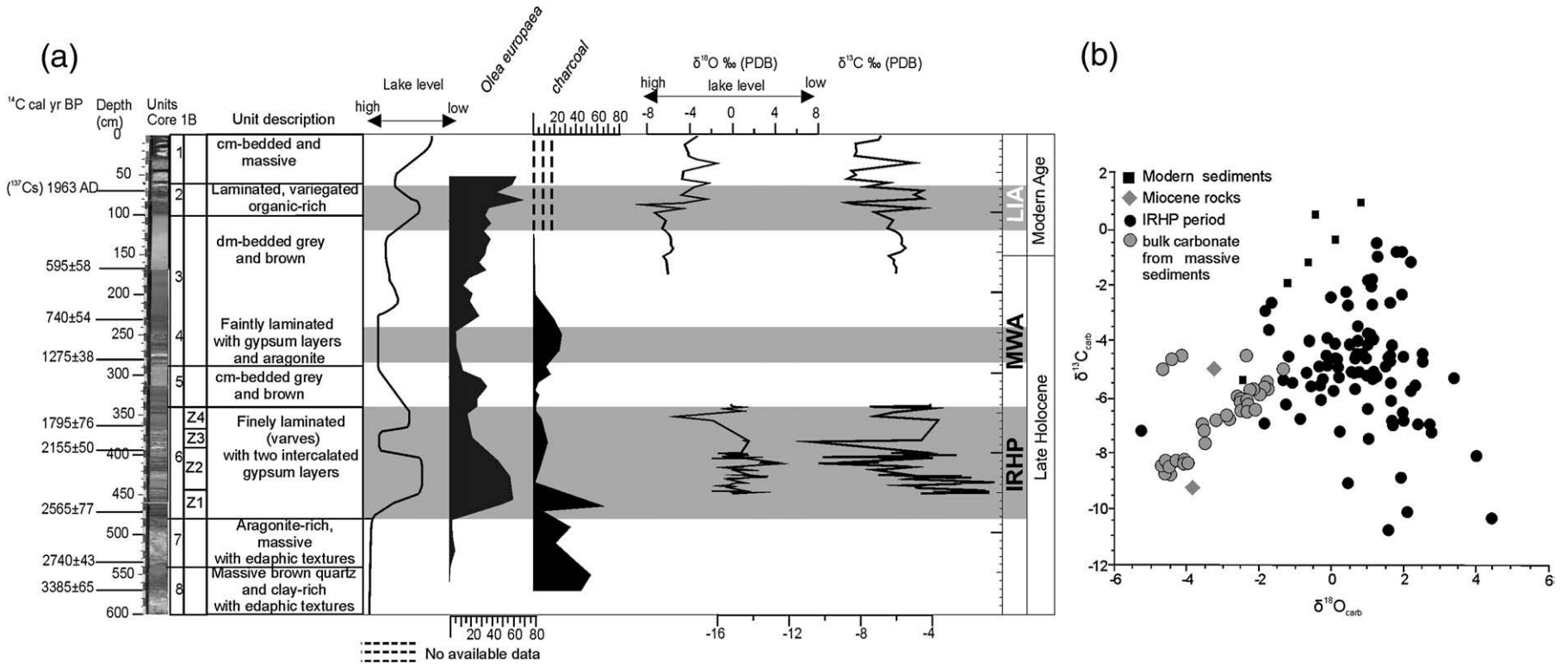

Figure 3. The late Holocene Zoñar record. Sedimentary units, AMS dates and inferred lake level (Martín-Puertas et al., 2008). *Olea* and charcoal profiles and isotopic composition of bulk carbonate sediments for core ZON04-1B. Humid periods are shown shaded. In the inset, cross plot of isotopic compositions of massive sediments (modern and late Holocene), watershed rocks and endogenic carbonates.

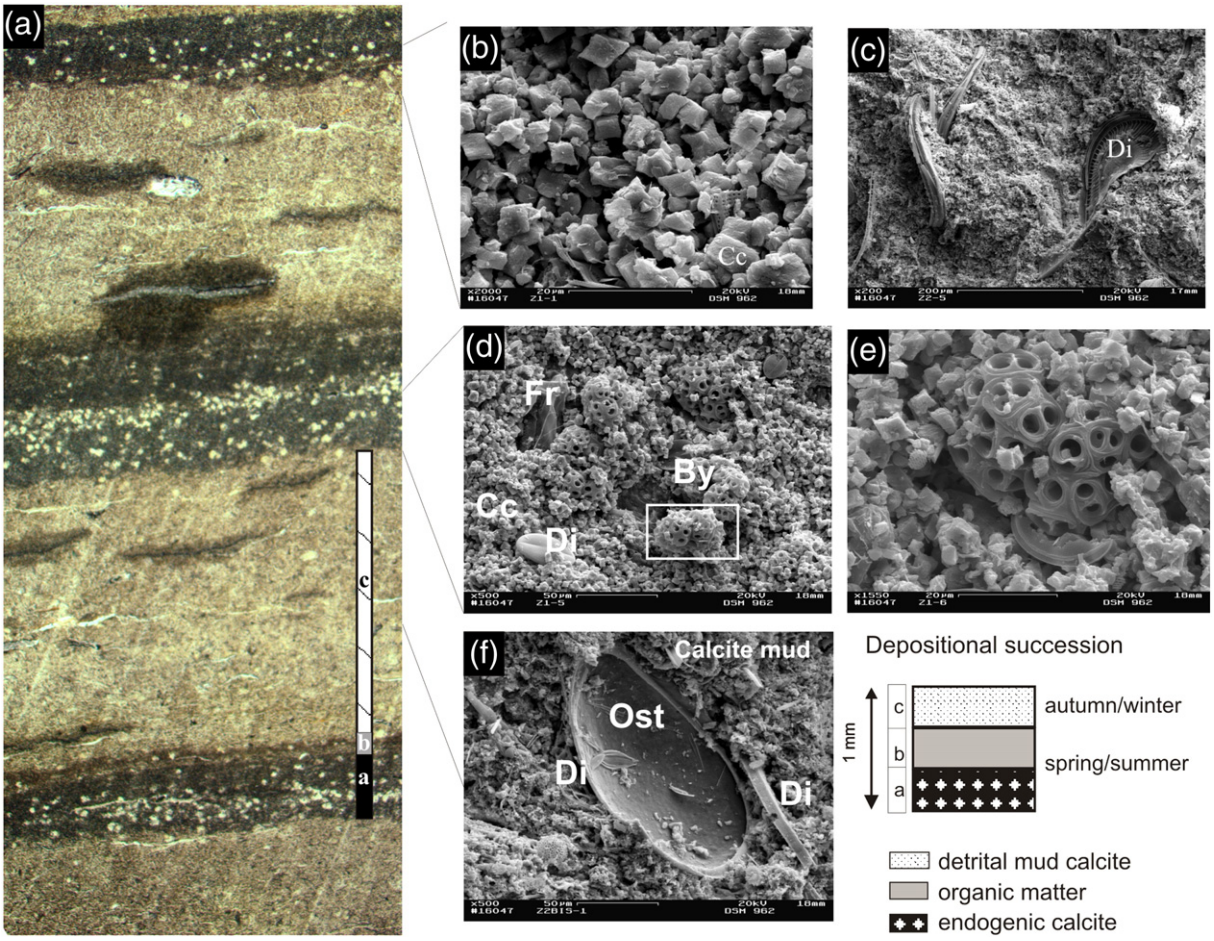

Figure 4. Thin section photos and electronic microscope images of Zoñar varved sediments, core ZON04-1B. (a) Microfacies 1a showing the three sublayers; (b) calcite crystals; (c) Organic sublayer with diatoms and amorphous organic matter; (d) calcite sublayer. Note the homogeneous size of the calcite crystals and the abundance of *Botryococcus*; (e) *Botryococcus* structure in detail; (f) detrital layer.

diatoms and algae filaments embedded by a greenish mucilage with some pyrite (<5%). This layer represents deposition of organic material during and after the algal blooms; and iii) a brownish *detrital layer* of calcite mud composed of irregular and rice-shaped calcite grains, clay minerals, silt-size quartz, fragment of diatoms and some terrestrial plant remains (Fig. 4c). This layer is interpreted as clastic deposition during the rainy season (fall and winter).

Four major micro-facies types have been identified (Table 1; Fig. 5a).

Table 1
Sedimentary microfacies identified in the IRHP period in Zoñar cores (ZON04-1B and ZON04-1C)

Micro-facies	Description	Sequences	Occurrence	Depositional environment
1. Well-preserved varves	Mm-thick laminated sediments are composed of three sublayers: calcite (5–15 μm crystals) organic (algal remains, diatoms) and detrital (mud and silt size). Varve thickness: 0.88–2. 3 mm (1a); 0.6–1, 2 mm (1b); 1.4–3. 5 mm (1c).	1a. Calcite (0.1–0. 8 mm)/organic matter (0.1–0.3) /detrital (0.8–1.5). Larger calcite grain size (10–15 μm). 1b.Organic matter (0.1–0.4)/detrital (0.4–0.9) 1c. Calcite (1.0–2.0)/detrital(0.4–1.5). Smaller calcite grain size (5–7 μm)	Zones 2, 3 and 4	Offshore areas, with anoxic bottom conditions (meromictic to monomictic lake) and lower detrital input. High lake level.
2. Poorly preserved varves	Similar to micro-facies 1a, but poorly preserved. calcite laminae occur as lenses, with wavy, non-parallel boundaries.	2. Calcite layer/organic matter/detrital. Thicker varves than 1 (around 4–6 mm)	Zones 1, 2 and 4	Offshore areas with suboxic bottom conditions (monomictic lake with more unstable mixing and oxic bottom water conditions) with relatively lower lake level and higher detrital input.
3. Event layers	Cm-bedded, massive coarse silt and sand sediments composed of calcite, quartz and clay minerals. Quartz grains size up to 2 mm. Diatom content is relatively high, many of them broken.	3a. Gray massive coarse carbonate silt with high quartz content (20%). 3b. Fining upward layer composed of a 10 cm thick sandy layer at the base and massive coarse silt with organic matter, gastropods and shells.	Zones 1 and 4	3a: Flood layers reaching offshore environments. 3b: "Transgressive" event: clastic deposition in sublittoral–offshore areas caused by an intense flooding period.
4. Gypsum layer	4a: Gypsum nodules composed of prismatic (80–140 μm long) gypsum crystals in a carbonate silt matrix 4b: Cm-thick layers made of prismatic (10–30 μm long) gypsum crystals.		Zone 3	4a. Gypsum formation in sediment interstitial waters 4b. Gypsum precipitation from chemically concentrated lake waters

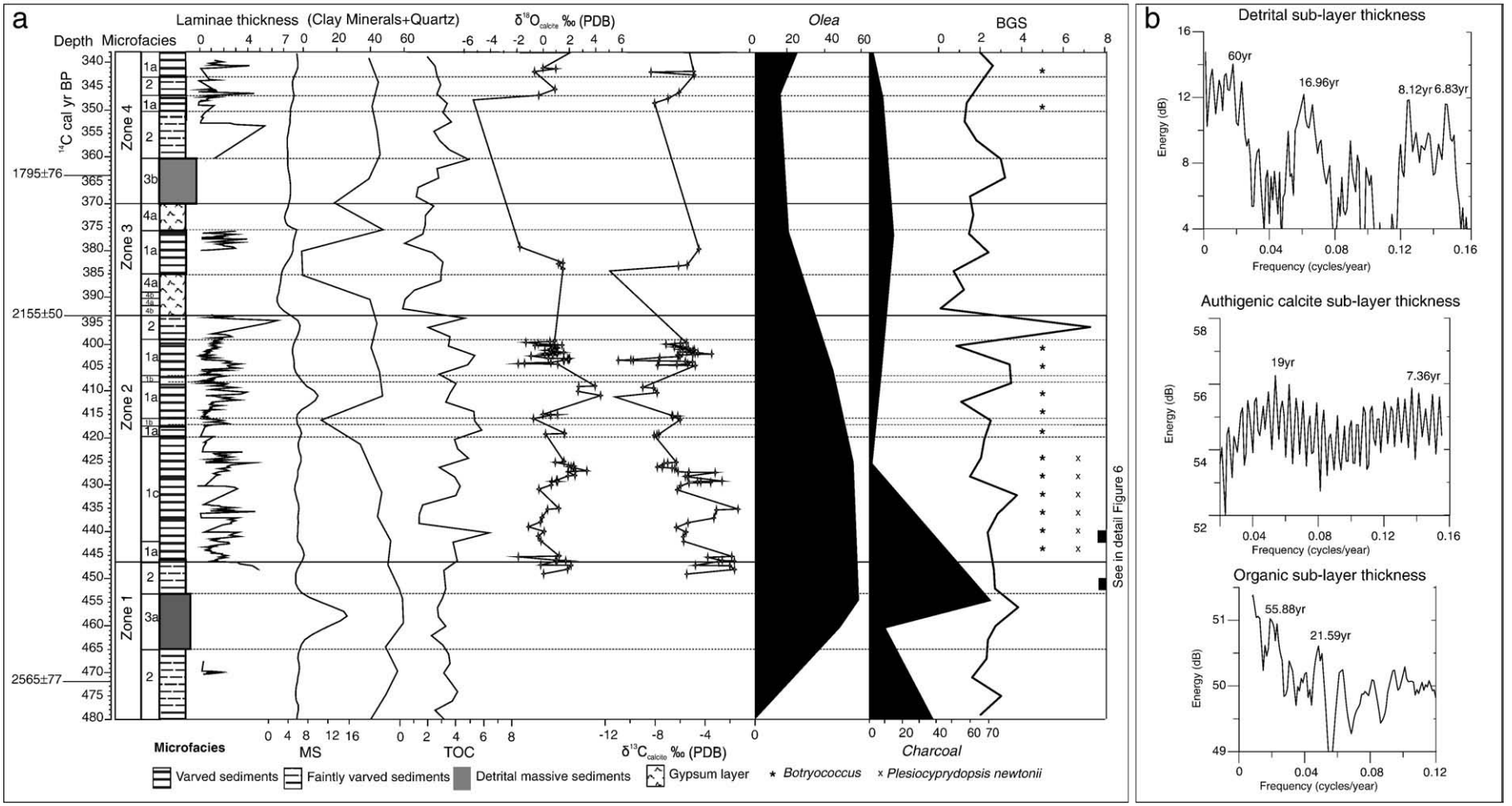

Figure 5. (a) Sedimentological, geochemical and biological indicators in the IRHP (core ZON04-1B). Sedimentary microfacies, laminae thickness, magnetic susceptibility, silicate detrital minerals (clays and quartz), organic carbon (TOC) isotopic composition of endogenic calcite layers and presence of *Botryococcus*. Data for biogenic silica (BGS), *Olea* pollen, charcoal and ostracods (*Plesiocyprydopsis newtonii*) from Martín-Puertas et al. (2008); (b) Spectrum analysis of detrital, endogenic calcite and organic sublayer thickness and the main cyclicity expressed as cycles per year for the IRHP. Spectra obtained from Lomb–Scargle Fourier transform using SPECTRUM (Schulz and Stattegger, 1997).

Microfacies 1 is a finely laminated varve deposit. The internal composition of microfacies 1 corresponds to the biogenic varve described by Brauer (2004) as formed by triplets of light (calcite), green brownish (organic) and dark (detrital) sub-layers (see above; Fig. 4). The large range of varve thickness (the sum of the three sub-layers) between 0.6 and 3. 5 mm (Table 1) indicates fluctuating environmental conditions (Brauer and Casanova, 2001), also reflected in the internal varve structure changes: microfacies 1a with all three sublayers, 1b without the calcite layer and 1c, without the organic layer (Table 1). The *Botryococcus* blooms only occur associated with the calcite sublayer (1a and 1c) at 2500–2165 cal yr BP (446–399 cm) and 1725–1600 cal yr BP (351–338 cm) intervals (Fig. 5a). Microfacies 1c is composed of thicker calcite layers (1–2 mm, Table 1), higher crystal density and smaller calcite grain size (5–7 μm) than microfacies 1a (0.1–0. 8 mm and 10–15 μm).

Interpretation: Microfacies 1 represents deposition in a pelagial, relatively deep lake bottom environment. The absence of any evidence of increased salinity in the hypolimnion (no presence of gypsum or other evaporite minerals) suggests that water stratification was achieved by increasing lake depth. The triplet facies are interpreted as deposited during periods of well-defined stratification more likely to occur in a meromictic lake or in a monomictic lake (annual water mixing) with prolonged periods of anoxic bottom sediments. Epilimnetic formation of calcite—'whiting' or seasonal clouding of lakes (Wright, 1990)—is typical of summertime in lakes located in carbonate bedrock areas (Zolitschka, 2003; Brauer et al., 2008). However, it may also occur during the onset of spring, even before the main algal blooms as in Lake Zurich (Kelts and Hsü, 1978), and in Lake Baldeggersee, Switzerland (Teranes et al., 1999a,b). *Botryococcus* blooms are most abundant after heavy rainfall, so they have been used as an indicator of freshwater input in lakes (Cane, 1976). Therefore, the calcite in Zoñar Lake likely precipitated as a consequence of temperature and pH rise in spring and associated with increased primary production by *Botryococcus* colonies; organic matter deposition (diatoms and other algal bloom) occurred in summer, and the detrital layer formed during the rainy months in late fall and winter. The triplets turn into couplets in microfacies 1b and 1c (Table 1), although they also represent an annual cycle. The absence of calcite layer during microfacies 1b indicates that conditions for calcite precipitation or preservation were not met. Calcite precipitation in microfacies 1c was also likely associated with biological activity as indicated by the occurrence of *Botryococcus* colonies remains, although thicker calcite laminae and smaller crystal size in microfacies 1c (calcite/detrital couplets) suggest that saturation conditions or organic productivity periods lasted longer (warmer summers) or that the amounts of calcium and bicarbonate ions in the waters were higher (increased supply due to higher winter precipitation and aquifer recharge) as shown in other Spanish lakes (Romero-Viana et al., 2008). Occurrence of larger calcite grain size as in microfacies 1a has been interpreted in other lakes (Teranes et al., 1999a,b) as precipitation during spring months responding to higher phosphate content. On the other hand, the absence of organic matter layer in microfacies 1c suggests there was only one annual algal bloom. The presence of ostracods (*Plesiocyprydopsis newtonii*) in microfacies 1c suggests less anoxic conditions in the bottom waters or shorter periods of anoxia than during deposition of microfacies 1a and 1b with no ostracod fauna (Martín-Puertas et al., 2008) (Fig. 5a).

Microfacies 2 is similar to microfacies 1 but varves are poorly preserved, *Botryococcus* remains are absent and laminae are thicker (Table 1).

Interpretation: faint lamination is associated with non permanent anoxic conditions in the bottom of the lake. The absence of *Botryococcus* suggests a change in seasonality with lower freshwater input during the early spring. However, the thicker detrital layer (compared to microfacies 1) suggests a greater rainfall that could have mostly occurred during the drier season (spring and summer) causing higher catchment erosion. In addition, more frequent holomixis in the lake waters is more easily attained in a lower lake level stage (Heim et al., 1997).

Microfacies 3 only occurs in two intervals, at the base and at the top of the laminated section. These are centimeter-thick layers composed of massive to graded coarse silt and sand sediments with abundant amorphous aquatic and terrestrial organic matter remains.

Interpretation: The high magnetic susceptibility values, high allochthonous mineral content and fining upward textures indicate the clastic nature of this microfacies and its deposition by high energy, current-dominated processes in the lake related to periods of more intense flooding in the watershed.

Microfacies 4 occurs as centimeter-thick gypsum layers intercalated in the laminated interval. There are two types: i) centimeter-thick layers of carbonate silt matrix with gypsum nodules (2–5 mm long nodules composed of 40–50 μm long gypsum crystals) and isolated, longer (80–140 μm) gypsum crystals (microfacies 4a), ii) 1.5–2 cm thick layers made of 100% gypsum crystals around 10–30 μm long, prismatic and randomly oriented (microfacies 4b) (Fig. 5a, Table 1). The contact with microfacies 2 is gradual with a 0. 5 cm zone with longer gypsum crystals (50 μm).

Interpretation: The pyramidal crystals shapes, the homogeneous crystal size, and the random distribution of the gypsum crystals in the microfacies 4b layers suggest gypsum precipitation within the water column (Smoot and Lowenstein, 1991), a consequence of chemically concentrated lake waters, and saturated conditions for sulfates. The textures of microfacies 4a indicate gypsum formation from the sediment interstitial brine waters (Cohen, 2003), that may occur in relatively "deep" and concentrated hypolimnetic waters in meromictic saline lakes (Last, 1994).

Cyclic lake environmental response

Spectral analysis based on the Lomb–Scargle Fourier transform for unevenly spaced data (Schulz and Stattegger, 1997) was performed in order to investigate the cyclicity of the lake response to environmental changes using varve sub-layer (calcite, detrital, organic) thickness (Fig. 5b). The power spectra for the three varve sub-layer thickness show multidecadal cycles with periods of ca. 60 and 20 years for the three types. This cyclicity is similar to modern North Atlantic Oscillation (NAO) patterns (Labat, 2006; de la Torre et al., 2007) and it suggests a climate control on distribution pattern of microfacies 1a and b.

XRF geochemistry

Micro-XRF analyses have been carried out in zone 2, where the varves are best preserved. The Al and K counts have a strong correlation (0.91), and also Fe with Al and K (0.8) suggesting feldspar, clay minerals and pyrite occurrence in those laminae as determined by micro-XRD, XRD and microscope observations. The Si/K ratio allows to distinguish biological and clastic sources and to identify individual diatom layers present in microfacies 1 and 2 through peak values (Figs. 6a, b).

The Ca and Sr counts in the varves are mainly related to carbonate, as shown by the negative correlation coefficient with the siliciclastic components (Al, K and Fe) (Fig. 6), and the abrupt peaks associated to the calcite laminae stressing the endogenic origin for calcite in these layers. Therefore, Ca/K can be used to detect the presence of varves in microfacies 2, where varve preservation is poor (Fig. 6b).

The S peaks are not associated with pyrite, but to the presence of colonies of green unicellular microalga *Botryococcus braunii*. This species is characterized by a high content of hydrocarbon and fatty acids (Maxwell et al., 1968) and also incorporates reduced inorganic sulfur species at early stages of diagenesis giving rise to organo-sulfur compound (OSC) (Grice et al., 2003). The positive correlation of Ca and S in microfacies 1a (Fig. 6a) further favors the hypothesis that biogenic calcite precipitation was induced by the *Botryococcus braunii* blooms (Figs. 4 and 7).

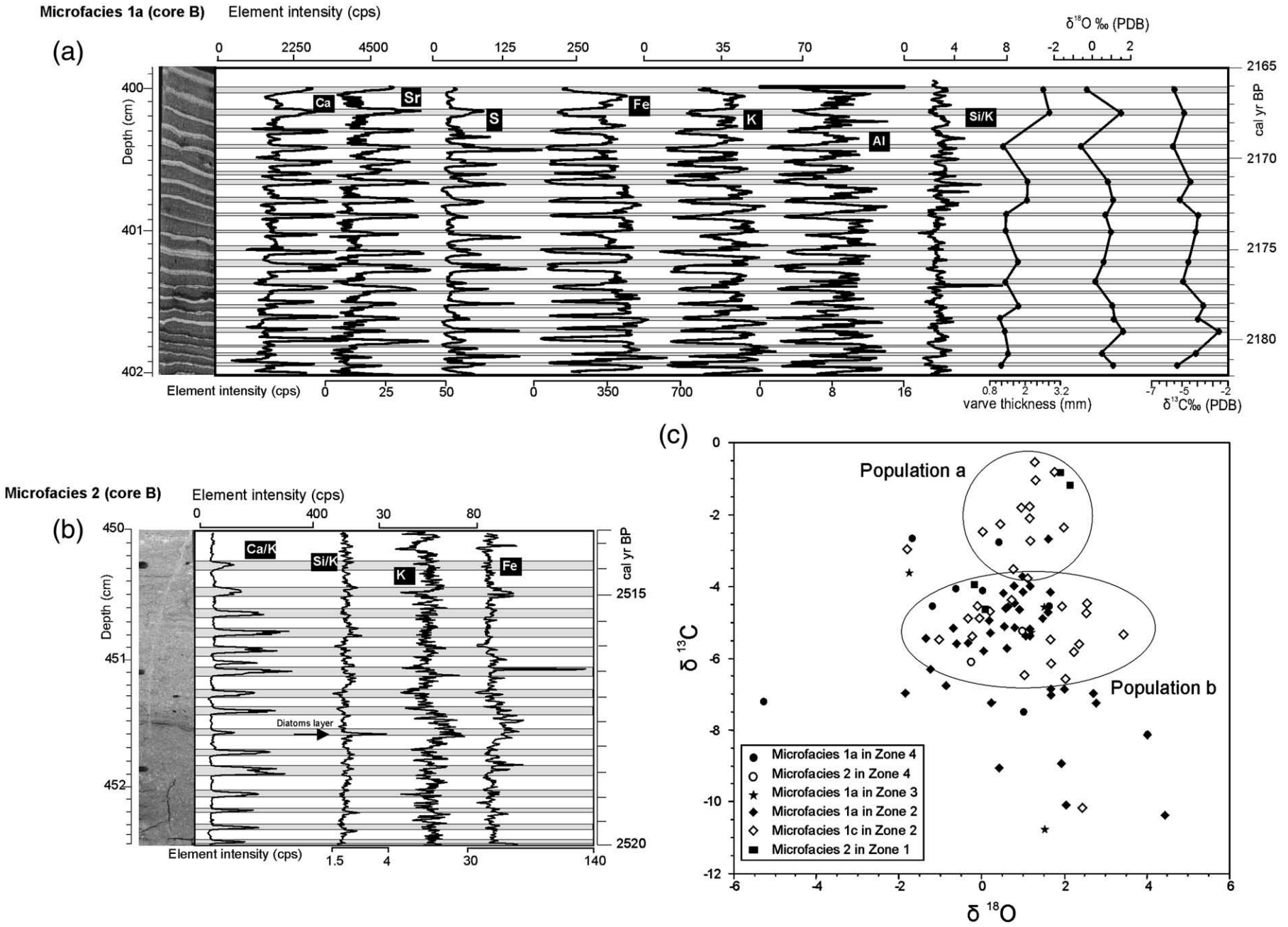

Figure 6. Micro geochemical composition and isotopic composition of endogenic calcite layers for the varved microfacies 1 and 2 in core ZON04-1B from zone 2 (a) and 1 (b). Calcite layer are marked by gray bands. (c). Cross plot of oxygen and carbon isotope composition of endogenic calcite from varves.

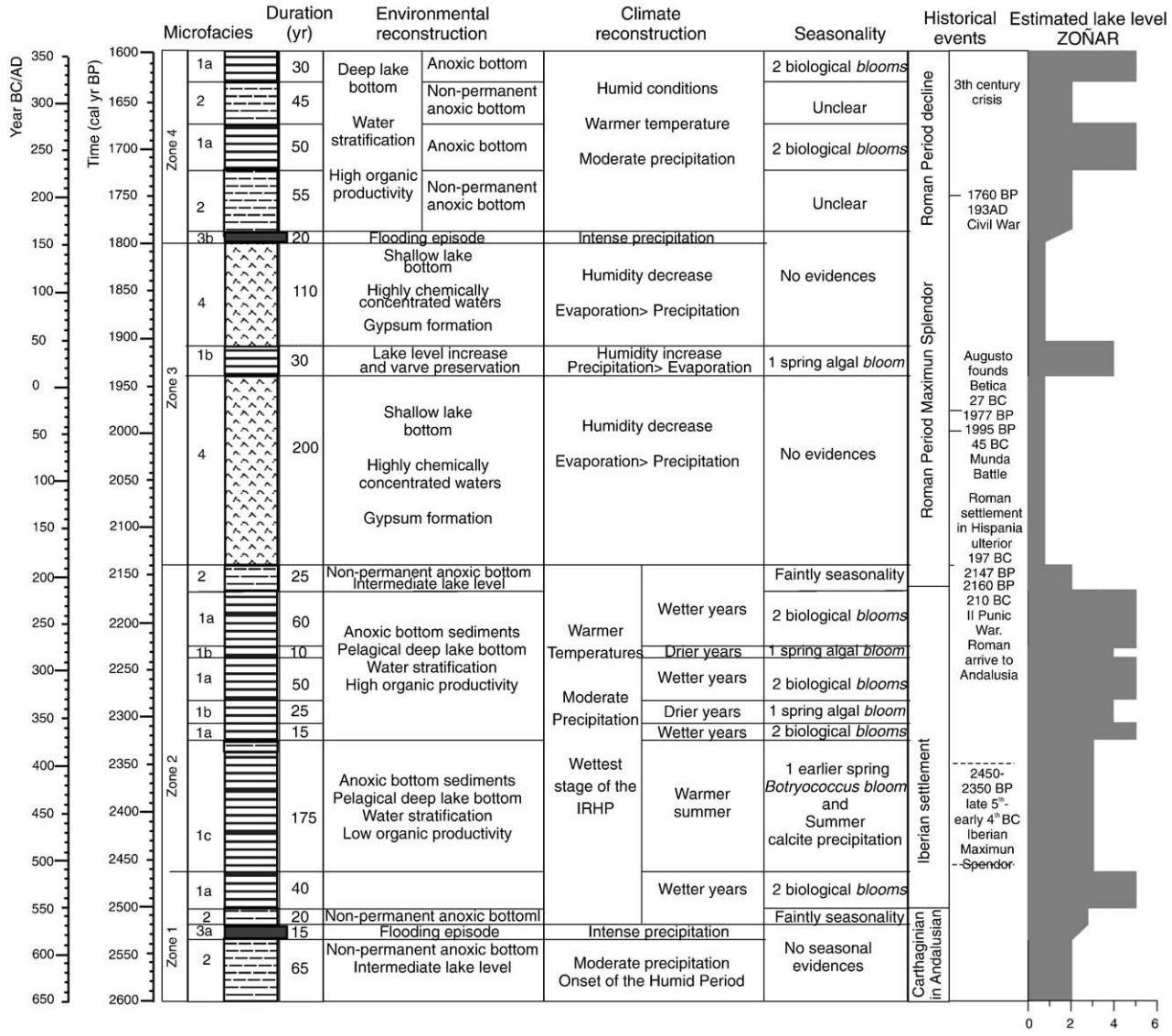

Figure 7. Environmental changes during the IRHP in Zoñar (lake level, cyclicity, seasonality) compared to historical events. Lake level reconstruction is based on hydrological interpretation of microfacies, so that 1a represents more humid conditions and higher lake level than 1b>1c>2>4; microfacies 3 is interpreted as flooding episodes and consequent lake level rise. (See text).

Stable isotope geochemistry

Isotopic values $\delta^{18}O$ of calcite precipitating in the surface waters of Zoñar Lake obtained from a buoy and anchor rope concretion growth show values (between −2 to +1‰ vs V-PDB) coherent with calcite formation in isotopic equilibrium with epilimnetic lake waters (+1 to + 6‰ $\delta^{18}O_{water\ (V\text{-}SMOW)}$) (Fig. 1c). The $\delta^{13}C_{calcite}$ and $\delta^{13}C_{DIC}$ show a similar compositional range (−3 to +2‰). Modern $\delta^{13}C_{DIC}$ values from the lake bottom waters have lighter isotopic compositions due to the absence of ^{13}C enrichment caused by photosynthesis and/or the input of ^{13}C depleted related with the oxidation of organic matter (Fig. 1c). Isotopic composition of bulk carbonate samples from the massive sedimentary units ($\delta^{18}O_{calcite}$ values from −1 to −5‰ vs V-PDB) shows distinctively lighter oxygen isotopic compositions than endogenic calcite laminae from the IRHP interval ($\delta^{18}O_{calcite}$ values from −2 to +4‰ vs V-PDB), and a smaller $\delta^{13}C_{calcite}$ range (between −4.5 and −9‰ for the bulk carbonates and −10.1 and −0.5‰ for laminites). Interestingly, the bulk carbonate samples show a clearer covariance pattern than the laminae samples, but this trend is more likely a reflection of the mixing of several carbonate sources (lighter detrital and heavier endogenic) and not to hydrological behavior of the lake (Fig. 3b).

The relatively high $\delta^{18}O_{calcite}$ values in the varves are coherent with calcite formation in the evaporatively—enriched epilimnetic waters, as in modern conditions. The measured values of $\delta^{18}O_{water}$ in modern surface samples show a large range (−2 to +5‰), reflecting variable evaporative conditions and freshwater inputs into the lake. On the other hand temperature changes could determine negative $\delta^{18}O_{calcite}$ excursions when calcite formation occurs in summer, in which case the positive excursions would indicate a higher proportion of spring calcite (lower water temperatures). However, the continuous enrichment of ^{18}O, due to evaporation, during spring and summer results in heavier isotope values at the end of the warm seasons. Consequently, the isotopic oscillations can be interpreted as a reflection of changes in the intensity of the evaporation processes (Li and Ku, 1997) that cancel out the opposite effect of the temperature increase (decreasing isotopic fractionation with increasing temperature; McCrea, 1950).

The $\delta^{13}C_{calcite}$ is mostly affected by carbon inputs to the lake, including exchange with the atmosphere, and biological activity, and secondarily by the hydrologic balance (Li and Ku, 1997). Lighter values are related with the oxidation of organic matter (internal or external) and inherited carbon from soil respiration (external DIC). Heavier $\delta^{13}C$

values are favored by increased evaporation, residence times (Li and Ku, 1997) and productivity (Leng and Marshall, 2004). Therefore the large range of $\delta^{13}C_{calcite}$ values in Zoñar samples is related to the numerous processes affecting the isotopic carbon cycle in lakes, but especially to surface processes (photosynthesis and respiration) and lake bottom processes (only respiration, resulting in very negative carbon from oxidation of organic matter).

The smaller calcite crystal size (5–8 μm) in microfacies 1c suggests that calcite precipitated associated with one major *Botryococcus* bloom in early summer, while larger calcite crystal sizes (10–15 μm) in microfacies 1a indicate spring and late fall calcite, as it has been interpreted in other lakes (Teranes et al., 1999a,b). In a cross plot (Fig. 6c) samples for microfacies 1c show two distinct populations: a) the highest $\delta^{13}C_{calcite}$ and relatively high $\delta^{18}O_{calcite}$, and b) moderate $\delta^{13}C_{calcite}$ and variable $\delta^{18}O_{calcite}$. The high $\delta^{13}C_{calcite}$ values indicate precipitation from ^{13}C enriched waters after preferential removal of ^{12}C from the DIC by primary producers (Mckenzie, 1982; Teranes et al., 1999a,b). Corresponding high $\delta^{18}O_{calcite}$ values and smaller calcite crystal size suggest that calcite precipitated later in the season related with the rapid and local pH increase due to the phytoplankton blooms. Calcite from microfacies 1a (zone 2) shows a similar $\delta^{18}O_{calcite}$ range as microfacies 1c but significantly lower $\delta^{13}C_{calcite}$ values (Fig. 5a). These more negative $\delta^{13}C$ values can be related to periods of a lower degree or an absence of lake water stratification that would have caused a higher input of the more negative DIC from the lake bottom waters (Fig. 1c). The anti covariant pattern displayed by the $\delta^{18}O_{calcite}$ and $\delta^{13}C_{calcite}$ curves in the lower part of microfacies 1a (zone 2, 442–446 and 405–420 cm) suggest that timing of calcite precipitation and CO_2 limitation could have been the main factors as shown in other lakes (Neumann et al., 2002). Calcite precipitated early in the season when evaporation effects were lower (low $\delta^{18}O_{calcite}$ values) during *Botryococcus* blooms would have the typical high $\delta^{13}C_{calcite}$ signal associated at high organic productivity. Calcite precipitated later in the season (summer), when surface waters are more evaporated (local increase in ^{18}O) and higher temperature and light favor photosynthesis (consumption of CO_2, decrease in superficial CO_2 concentration), would have higher $\delta^{18}O_{calcite}$ and $\delta^{13}C_{calcite}$ values. Limnological conditions changed in the upper part of zone 2 (394–399 cm) and the $\delta^{18}O_{calcite}$ and $\delta^{13}C_{calcite}$ display again similar trends. This pattern could be explained by more intense *Botryococcus* blooms (high S content, Fig. 4) when spring rainfall occurs earlier in the season.

The IRHP humid period in the European context

The time interval from 2600 to 1600 cal yr BP is the most humid period in Zoñar Lake and is synchronous with other records of increased water availability in Spain around the same time: a marine core from Northwestern Iberia (Desprat et al., 2003); lake records from southern-central Spain (Gil-García et al., 2007), geomorphological (Gutierrez-Elorza and Peña-Monne, 1998), fluvial (Macklin et al., 2006) and $\delta\ ^{13}C$ of archaeological charcoal (3450–2850 and 2250–1650 cal yr BP) evidences in the Ebro Basin (Ferrio et al., 2006) among others. The chronological model and the high resolution data allow a more detailed paleolimnological reconstruction of Lake Zoñar during the IRHP. A qualitative lake level curve was reconstructed based on the hydrological interpretation of microfacies and the integration of the geochemical and biological data for the varved interval (Fig. 7). Microfacies are arranged according with the interpreted paleobathymetry of their depositional environment from deeper to shallower as follows: 1a>1b>1c>2>4; microfacies 3 is interpreted as flooding episodes and consequent lake level rise. Based on microfacies data and their limnological interpretation four main stages can be identified (Fig. 7).

Zone 1, 2600–2500 cal yr BP/650–550 BC (480–446 cm). Deposition of microfacies 2 represents the onset of a period of higher humidity after a late Holocene arid period well documented in the Mediterranean Basin and Europe (Lamb et al., 1995; Issar, 2003). Deposition of microfacies 3a (2535–2520 cal yr BP) marks a lake transgressive event likely caused by a period of intense flooding. After the deposition of this layer, limnological conditions changed progressively and were more conducive to varve formation and preservation, with relatively stable lake environments, deep enough to establish summer stratification leading to anoxic bottom conditions (microfacies 2).

Zone 2, 2500–2140 cal yr BP/550–190 BC (446–392 cm), is characterized by permanent stratification, except in the upper part where seasonal stratification and more frequent holomictic conditions occurred (microfacies 2). After an initial deposition of microfacies 1a for a few decades (2500–2460 cal yr BP/550–510 BC), deposition of microfacies 1c (calcite/detrital couplets) dominated for about 135 yr (2460–2325 cal yr BP/510–375 BC) in a stable deep lake with anoxic bottom sediments and relatively low organic productivity. Isotopic and textural data support this scenario of warmer temperatures, moderate precipitation during late winter and early spring and only one summer *Botryococcus* bloom. Conditions changed around 2325 cal yr BP to an alternation of longer periods (around 60 yr) of deposition of microfacies 1a (spring calcite formation, longer blooms) and shorter periods (around 10–30 yr) of microfacies 1b (organic/detrital). This 180 yr long period of strongest seasonality, represents the most productive interval in the IRHP. Higher precipitation in cold winter caused *Botryococcus* bloom in spring and a secondary algal bloom occurred later in the season (microfacies 1a); during drier years with predominant springtime precipitation, only one algal bloom occurred likely in late spring (microfacies 2) (Fig. 7). These moisture changes (alternation of microfacies 1a and 1b) are of similar frequency as those documented from meteorological data during the last decades in the region (Fig. 1a) and colder /wetter winters with drier summers interpreted for the period 900–300 BC in the Ebro Basin (Ferrio et al., 2006).

The most humid period coincides with the development of Iberian settlements in the region (Cordoba province) during late 5th and early 4th centuries BC (Chapa Brunet, 1998) (Fig. 7). The timing is synchronous with the *Olea* (60%) and charcoal peaks in the Zoñar record (Fig. 3), both suggesting anthropogenic influence and a possible cultivation prior to Roman colonization. Other sites in southern Spain (Baza) show a strong human impact after 2600 cal yr BP (Carrión et al., 2007). Similar evidences have been shown in Italy during the 2700–2190 cal yr BP when *Olea* pollen percentages (>20%) were higher than during previous periods (Caroli and Caldara, 2007) and increased fire frequency has been linked to local human presence (Lago Battaglia, Italy, Caroli and Caldara, 2007 and Lago Accesa, Italy, Vannière et al., 2008). The onset of the strong Roman influence in Andalusia, at 210 BC (2160 cal yr BP) correlates with the beginning of a decreasing lake level trend, more frequent holomictic conditions and deposition of microfacies 2 at 2180 cal yr BP. Despite good general agreement, comparison with Central Mediterranean lake level reconstructions (Magny et al., 2007) and the Spanish flood record (Macklin et al., 2006) at decadal scale reveals slight differences for the period from 2300 to 2150 cal yr BP (Fig. 8) when the Zoñar lake level was still high, whereas flooding frequency in Spain and lake level in Italy decreased. These discrepancies may indicate processes associated to seasonality changes and also the chronological uncertainties associated to the hydrological reconstruction of the Mediterranean lakes, as indicated by Magny et al. (2007) (Fig. 8).

Zone 3, 2140–1800 cal yr BP/190 BC–150 AD (392–367 cm), represents a sharp limnological change in Zoñar Lake leading to highly chemically concentrated waters (gypsum formation). This period appears slightly later than the decrease in flooding episodes and river activity in Spain during 2350–2000 cal yr BP (Macklin et al., 2006; Magny et al., 2002), but coincides well with the end of a wet period at 2100 cal yr BP in northern Europe (Aaby, 1976). Although several Mediterranean records show evidences of large hydrological changes in lakes during Roman times, it is not clear if those were induced by

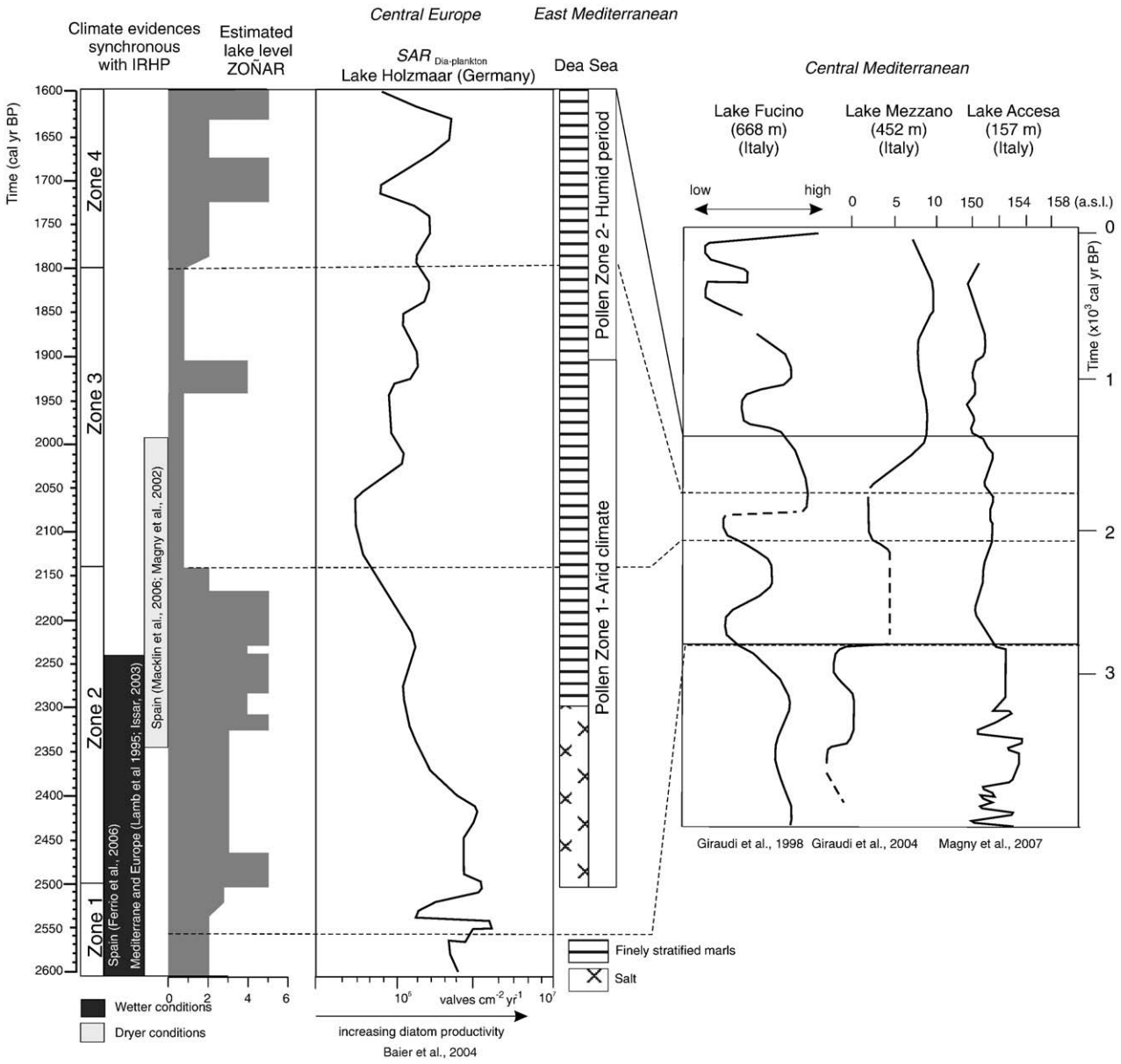

Figure 8. Paleohydrological comparison between Zoñar Lake and selected eastern and central Mediterranean and northern European lakes. The planktonic diatom in Lake Holzmaar has been interpreted as an indicator of paleoproductivity and paleohydrology (Baier et al., 2004). Lake Fucino, Lake Mezzano and Lake Accesa (Italy, central Mediterranean) records from Magny et al. (2007). Dead Sea hydrological reconstruction is based on sedimentary facies and pollen (modified from Heim et al., 1997).

either climatic variability or human use of the water or a combination of both factors. Magny et al. (2007) show a correlation between lake level inferred for several Italian lakes (Lake Fucino in Giraudi, 1998, Lake Mezzano in Giraudi, 2004 and Lake Accesa in Magny et al., 2007) and advances of alpine glaciers and concluded that, at a centennial scale, climate was the main control of the lake hydrology. This could have been the case for Lake Accesa where a relative lake level decrease occurred around 2100–1900 cal yr BP. However, in other lakes as Fuccino and Mezzano, intense Roman activity during the first and second centuries AD (1950–1750 cal yr BP) has been considered the main cause for partial drainage of both lakes (Giraudi, 1998). In other regions of Italy and Greece (Paepe, 1984; Reale and Dirmeyer, 2000) there have also been documentations of a decrease in lake levels during some periods of the Roman Epoch likely caused by increased water demand during drier conditions.

After the Munda Battle in 45 yr BC (Fig. 7), the Betica province was established by Augusto in southern Hispania (Bermejo, 2007) and human activities increased in the Zoñar area. However, the available pollen record shows a decrease in *Olea* and a relatively small charcoal peak associated with this gypsum rich interval (Fig. 3) and the lake level drop in Zoñar is synchronous to a regional episode of lower lake levels from 2100 to 1800 cal yr BP (Magny et al., 2007) suggesting that climate could have been the main driving factor, although human pressure could have increase the effects on Zoñar lake hydrology.

Zone 4, 1800–1600 cal yr BP/150–350 AD (367–338 cm) is characterized by a return to more humid conditions after a flood event (microfacies 3b). During this period called the 3rd century crisis (AD 235–285) (Vogt, 1968), the Roman Empire declined, and olive groves and villages were abandoned. A decrease in human impact in the watershed is indicated by lower *Olea* and charcoal pollen percentages (Fig. 3). During this period in the Zoñar record, climate fluctuations are defined by 60 yr cycles of laminated microfacies 1. Considering the modern climate patterns, microfacies 1a deposition

(relatively higher lake level, seasonal or permanent stratification) could reflect higher precipitation and microfacies 2 periods of lake level decrease (holomixis to seasonal stratification) during drier phases (Fig. 7).

The IRHP (2600–1600 cal yr BP) is broadly synchronous with the late Holocene wet/cool period that started at around 2800 cal yr BP in Europe and elsewhere (Bond and Lotti, 1995 based on ice-rafting events; Van Geel et al., 1996 from archaeological and paleoecological evidences; Beer et al., 1998 ice cores record in the North Atlantic ocean; Stuvier et al., 1997 oxygen isotope records from Greenland ice cores; Magny et al., 2002 based on lake level fluctuation). There is likely a connection between the IRHP onset and the well-established 2800–2710 cal yr BP abrupt climate change event that coincides with a $\Delta^{14}C$ increase in the atmosphere as a consequence of reduced solar output (Van Geel et al., 1996, 1999; Speranza et al., 2002).

Comparison with available records from northern Europe (Baier et al., 2004) and the Eastern Mediterranean (Heim et al., 1997) suggests that the IRHP was a European event, although it could have been shorter in the Western Mediterranean (Fig. 8). Baier et al. (2004) identified in varved lake sediments in Central Europe (Germany), three zones during the 2800–1470 cal yr BP cool and wet period: 2800–2220 cal yr BP and 1730–1470 cal yr BP were dominated by planktonic diatom species while benthic species increased during 2220–1730 cal yr BP. The onset of the IRHP in Zoñar is also synchronous to the beginning of the wet period in the Dead Sea cores (Heim et al., 1997), although the wet period lasted longer in the Eastern Mediterranean (Fig. 8).

The two main IRHP cycles (60 and 20 yr) are associated with microfacies shifts and therefore changes in seasonality: the average duration of period with predominant deposition of microfacies 1a, 1c and microfacies 2 (in zone 4) is around 60 yr, while for microfacies 1b the duration is ~20 yr. These cycles are similar to those defined in modern conditions and associated with NAO influence (60 yr, Labat, 2006) and the global oceanic thermohaline circulation (20 yr, Delworth and Greatbatch, 2000). Jones et al. (2006) documented a similar cyclicity (58 and 33 yr) in a Turkish lake record during two arid periods, 1650–1450 cal yr BP and 500 cal yr BP to present, and linked this variability to the Indian monsoon system. Although eastern and western Mediterranean regions may respond to different climate patterns at a decadal scale, the concordance of the variability between the Turkish and Spanish sites, during opposite moisture conditions supports a similar major climate forcing (e.g., changes in solar radiance). Finally, the >10 yr short-term oscillations during the IRHP are a reflection of the 11-year solar activity cycle during the Holocene (Theissen et al., 2008).

Conclusions

The Iberian–Roman Humid Period identified in the South of the Iberian Peninsula coincides with a global climatic phase that started with the 2.8 ka wet and cool event and was controlled by solar forcing. The onset of this period was gradual (2600–2460 cal yr BP) and the most humid interval occurred during the Iberian–Early Roman Epoch (2460–2140 cal yr BP).

An arid interval during the Roman Empire Epoch (2140–1800 cal yr BP) was caused by climatic forcing, but its limnological impact could have been increased due to higher anthropogenic impact on the lake system caused by lake water usage; a final humid phase occurred during the decline of the Roman Empire (1800–1600 cal yr BP). Similarities with northern European and Eastern Mediterranean records emphasize the northern hemispheric nature of this humid period, although the onset and decline may have been time transgressive. Evidences of moisture cycles of 60 and 20 yr in the Zoñar record are most significant during this period, suggesting a similar centennial long-term NAO correlation as in modern climate.

Archaeological data in central and southern Europe show that human settlements during the IRHP were favored by moist climate conditions. In southern Spain, this period coincides with the flourishing of the Iberian culture and the Roman conquest.

Acknowledgments

Financial support for this study was provided by the Spanish Ministry of Science and Education (projects LIMNOCLIBER REN 2003-09130-CO2-02, IBERLIMNO CGL2004-20236-E, CALIBRE CGL2006-13327-C04/CLI, CGL-2006-2956-BOS and CGL2007- 65572- CO2- 01), Andalusian Government Predoctoral Fellowship and the Andalusian Government (PAI group RNM-328, RNM- 309 and project P06- RNM-02362). We thank Penélope González-Sampériz for pollen identification and interpretation. We are grateful to Suzanne Leroy, an anonymous reviewer and the editors David J. Meltzer and Alan Gillespie for their criticisms and suggestions that improved the manuscript. Finally we thank LRC (University of Minnesota, USA), and particularly to Doug Schnurrenberger, Mark Shapley and Anders Noren for making possible the 2004 expedition. We gratefully acknowledge funding from DAAD (German Academic Exchange Programme) and the Acciones Integradas Hispano-Alemanas Project D/07/13363.

References

Aaby, B., 1976. Cyclic climatic variations in climate over the past 5,500 yr reflected in raised bogs. Nature 263, 281–284.
Audino, M., Grice, K., Alexander, R., Bareham, C.J., Kagi, R.I., 2001. An unusual distribution of monomethylalkanes in *Botryococcus braunii*-rich sediments. Their origin and significance. Geochimica et Cosmochimica Acta 12, 1995–2006.
Baier, J., Lücke, A., Negendank, J.F.W., Schleser, G.H., Zolitschka, B., 2004. Diatom and geochemical evidence of mid- to late Holocene climatic changes at Lake Holzmaar, West-Eifel (Germany). Quaternary International 113, 81–96.
Baroni, C., Zanchetta, G., Fallick, A.E., Longinelli, A., 2006. Mollusca stable isotope record of a core from Lake Frassino, northern Italy: hydrological and climate changes during the last 14 ka. The Holocene 16, 827–837.
Beer, J., Siegenthaler, U., Bonani, G., Finkel, R.C., Oeschger, H., Sutter, M., Wölfli, W., 1998. Information on past solar activity and geomagnetism from ^{10}Be in the Camp Century ice core. Nature 331, 675–679.
Bermejo, J., 2007. Breve Historia de los Iberos. Imprenta Fareso, Madrid.
Bond, G., Lotti, R., 1995. Iceberg discharges into the North Atlantic on millennial time scales during the last glaciation. Science 267, 1005–1010.
Brauer, A., 2004. Annually laminated sediments and their paleoclimate relevance. In: Fischer, H., Kumke, T., Lohmann, G., Flöser, G., Miller, H., von Storch, H., Negendank, J.F.W. (Eds.), The Climate in Historical Times. Towards a Synthesis of Holocene Proxy Data and Climate Models. Springer Verlag, pp. 111–129.
Brauer, A., Casanova, J., 2001. Chronology and depositional processes of the laminated sediment record from Lac d'Annecy, French Alps. Journal of Paleolimnology 25, 163–177.
Brauer, A., Mangili, C., Moscariello, A., Witt, A., 2008. Palaeoclimatic implications from micro-facies data of a 5900 varve time series from the Pianico interglacial sediment record, Southern Alps. Palaeogeography Palaeoclimatology, Palaeoecology, 259, 121–135.
Cane, R.F., 1976. The origin and formation of oil shale. In: Yen, T.F., Chilingarian, G. V. (Eds.), Oil Shale. Developments in Petroleum Science, Elserviver, Amsterdam, pp. 27–60.
Caroli, I., Caldara, M., 2007. Vegetation history of Lago Battaglia (eastern Gargano coast, Apulia, Italy) during the middle-late Holocene. Vegetation History and Archaebotany 16, 317–327.
Carrión, J., Fuentes, N., González-Sampériz, P., Sánchez Quirante, L., Finlaysson, C., Fernández, S., Andrade, A., 2007. Holocene environmental change in a montane region of southern Europe with a long history of human settlement. Quaternary Science Reviews 26, 1455–1475.
Chapa Brunet, T., 1998. Iron age Iberian sculptures as territorial markers: the Córdoba example (Andalusía). European Journal of Archaeology 1, 71–90.
Cohen, A.S., 2003. Paleolimnology. The History and Evolution of Lake Systems. Oxford University Press, Oxford.
De La Torre, L., Gimeno, L., Añel, J.A., Nieto, R., 2007. The role of the solar cycle in the relationship between the North Atlantic Oscillation and Northern Hemisphere surface temperatures. Advances in Atmospheric Sciences 24, 191–198.
Delworth, T.L., Greatbatch, R.J., 2000. Multidecadal thermohaline circulation variability driven by atmospheric surface flux forcing. Journal of Climate 13, 1481–1495.
Desprat, S., Sanchez Goñi, M.F., Lourre, M.F., 2003. Revealing climate variability of the last three millennia in northwestern Iberia using pollen influx data. Earth and Planetary Science Letters 213, 63–78.

Enadimsa, 1989. Estudio hidrogeológico de la Laguna de Zoñar. Junta de Andalucía. Agencia de Medio Ambiente, Sevilla.
Ferrio, J.P., Alonso, N., López, J.B., Araus, J.L., Voltas, J., 2006. Carbon isotope composition of fossil charcoal reveals aridity changes in the NW Mediterranean Basin. Global Change Biology 12, 1–14.
Gil-García, M.J., Ruiz Zapata, M.B., Santisteban, J.I., Mediavilla, R., López-Pamo, E., Dabrio, C.J., 2007. Late Holocene environments in Las Tablas de Daimiel (south central Iberian peninsula, Spain). Vegetation History Archaeobotany 16, 241–250.
Giraudi, C., 1998. Late Pleistocene and Holocene lake-level variations in Fucino Lake (Abruzzo, central Italy) inferred from geological archaeological and historical data. In: Harrison, S.P., Frenzel, B., Huckried, U., Weiss, M. (Eds.), Palaeohydrology as Reflected in Lake-Level Changes as Climatic Evidence for Holocene Times, Palaoklimaforschung, pp. 1–17.
Giraudi, C., 2004. Le oscillazioni di livello del Lago di Mezzano (Valentino-VT): variazioni climatiche e interventi antropici. Il Quaternario 17, 221–230.
Grice, K., Schouten, S., Blokker, P., Derenne, S., Largeau, C., Nissenbaum, A., Sinninghe Damste, J.S., 2003. Structural and isotopic analysis of kerogens in sediments rich in free sulfurised *Botryococcus braunii* biomarkers. Organic Geochemistry 34, 471–482.
Gutierrez-Elorza, M., Peña-Monné, J.L., 1998. Geomorphology and late Holocene climate change in northeastern Spain. Geomorphology 23, 205–217.
Heim, C., Nowczyk, N.R., Negendank, J.F.W., 1997. Near east desertification: evidence from the Dead Sea. Naturwissenschaften 84, 398–401.
Issar, A.S., 2003. Climate Changes During the Holocene and their Impact on Hydrological Systems. Cambridge University Press, Cambridge.
Jones, M.D., Roberts, C.N., Leng, M.J., Türkes, M., 2006. A high-resolution late Holocene lake isotope record from Turkey and links to North Atlantic and monsoon climate. Geology 34, 361–364.
Juliá, R., Burjachs, F., Dasí, M.J., Mezquita, F., Miracle, J.R., Roca, G., Seret, G., Vicente, E., 1998. Meromixis origin and recent trophic evolution in the Spanish mountain lake La Cruz. Aquatic Sciences 60, 279–299.
Kelts, K., Hsü, K.J., 1978. Freshwater carbonate sedimentation. In: Lerman, A. (Ed.), Lakes: Chemistry, Geology, Physics. Springer-Verlag, New York, pp. 295–325.
Komárek, J., Marvan, P., 1992. Morphological differences in natural populations of the genus *Botryococcus* (Chlorophuceae). Arch. Protistenkd 141, 65–100.
Labat, D., 2006. Oscillations in land surface hydrological cycle. Earth and Planetary Science Letters 242, 143–154.
Lamb, H.F., Gasse, F., Benkaddour, A., El Homauti, N., van der Kaars, S., Perkins, W.T., Pearce, N.J., Roberts, C.N., 1995. Relation between century-scale Holocene arid intervals in tropical and temperature zones. Nature 373, 134–137.
Last, W.M., 1994. Deep-water evaporate mineral formation in lakes of Western Canada. In: Renaut, R.W., Last, W.M. (Eds.), Sedimentology and Geochemistry of Modern and Ancient Saline Lakes. Soc. Econ. Paleo. Mineral. Spec. Publ., 50, pp. 51–59.
Leng, M.J., Marshall, J.D., 2004. Palaeoclimate interpretation of stable isotope data from lake sediment archives. Quaternary Science Reviews 23, 811–831.
Li, H.-C., Ku, T.-L., 1997. δ13C-δ18O covariance as a paleohydrological indicator for closed-basin lakes. Palaeogeography, Palaeoclimatology, Palaeoecology 133, 69–80.
Luterbacher, J., Xoplaki, E., Casty, C., Wanner, H., Pauling, A., Küttel, M., Rutishauser, T., Brönnimann, S., Fischer, E., Fleitmann, D., González-Rouco, F.J., García-Herrera, R., Barriendos, M., Rodrigo, F., Gonzalez-Hidalgo, J.C., Saz, M.A., Gimeno, L., Ribera, P., Brunet, M., Paeth, H., Rimbu, N., Felis, T., Jacobeit, J., Dünkeloh, A., Zorita, E., Guiot, J., Türkes, M., Alcoforado, M.J., Trigo, R., Wheeler, D., Tett, S., Mann, M.E., Touchan, R., Shindell, D.T., Silenz, S., Montagna, P., Camuffo, D., Mariotti, A., Nanni, T., Brunetti, M., Maugeri, M., Zerefos, C., De Zolt, S., Lionello, P., 2006. Mediterranean climate variability over the last centuries: a review. In: Lionello, P., Malanotte-Rizzoli, P., Boscolo, R. (Eds.), The Mediterranean Climate: An Overview of the Main Characteristics and Issues. Elsevier, Amsterdam, pp. 27–148.
Macklin, M.G., Benito, G., Gregory, K.J., Johnstone, E., Lewin, J., Michczyńska, D.J., Soja, R., Starkel, L., Thorndycraft, V.R., 2006. Past hydrological events reflected in the Holocene fluvial record of Europe. Catena 66, 145–154.
Magny, M., Miramont, C., Sivan, O., 2002. Assessment of impact of climate and anthropogenic factors on Holocene Mediterranean vegetation in Europe on the basis of paleohydrological records. Paleogeography, Paleoclimatology, Paleoecology 186, 47–59.
Magny, M., de Beaulieu, J.-L., Drescher-Schneider, R., Vannière, B., Walter-Simonnet, A.-V., Miras, Y., Millet, L., Bossuet, G., Peyron, O., Brugiapaglia, E., Leroux, A., 2007. Holocene climate changes in the central Mediterranean as recorded by lake-level fluctuations at Lake Accesa (Tuscany, Italy). Quaternary Science Reviews 26, 1736–1758.
Martín-Puertas, C., Valero-Garcés, B.L., Mata, M.P., González-Sampériz, P., Bao, R., Moreno, A., Stefanova, V., 2008. Arid and humid phases in the southern Spain during the last 4000 years: the Zoñar Lake record, Córdoba. The Holocene 18, 907–921.
Maxwell, J.R., Douglas, A.G., Eglinton, G., McCormick, A., 1968. The Botyococcenes-hydrocarbons of novel structure from the alga *Botryocuccus Braunii*, Kützong. Phytochemistry 7, 2157–2171.
McCrea, J.M., 1950. On the isotopic chemistry of carbonates and palaeo-temperature scale. Journal of Chemical Physics 18, 849–857.
McKenzie, J.A., 1982. Carbon-13 cycle in Lake Greifen: a model for restricted ocean basins. In: Schlanger, S.O., Cita, M. (Eds.), Nature and Origins of Cretaceous Carbon-Rich Facies. Academic, pp. 197–208.
Moya, J.L., 1986. Análisis del hidrograma del manantial deZoñar. Oxyura 3, 29–33.
Myrbo, A., Shapley, M.D., 2006. Seasonal water-column dynamics of dissolved inorganic carbon stable isotopic compositions (δ13CDIC) in small hardwater lakes in Minnesota and Montana. Geochimica et Cosmochimica Acta 70, 2699–2714.
Neumann, T., Stögbauer, A., Walpersdorf, E., Stüben, D., Kunzendorf, H., 2002. Stable isotopes in recent sediments of Lake arendsee, NE Germany: response to eutrophication and remediation measures. Palaeogeography, Palaeoclimatology, Palaeoecology 178, 75–90.
Paepe, L., 1984. Landscape changes in Greece as a result of changing climate during the Quaternary in Desertification in Europe. In: Fantechi, R., Margaris, X. (Eds.), Proceedings of the International Symposium in the EEC Programme on Climatology. Reidel, Doudrecht, pp. 2–25.
Reale, O., Dirmeyer, P., 2000. Modeling the effects of vegetation on Mediterranean climate during the Roman Classical Period. Part I: climate history and model sensitivity. Global and Planetary Change 25, 163–184.
Reimer, P.J., Baillie, M.G.L., Bard, E., Bayliss, A., Beck, J.W., Bertrand, C., Chanda, J.H., Blackwell, P.G., Buck, C.E., Burr, G.S., Cutler, K.B., Damon, P.E., Edwards, R.L., Fairbanks, R.G., Friedrich, M., Guilderson, T.P., Hogg, A.G., Hughen, K.A., Kromer, B., McCormac, G., Manning, S., Ramsey, C.B., Reimer, R.W., Remmele, S., Southton, J.R., Stuiver, M., Talamo, S., Taylor, F.W., van der Plicht, J., Weyhenmeyer, C.E., 2004. IntCal04 Terrestrial radiocarbon age calibration, 0–26 cal Kyr BP. Radiocarbon 46, 1029–1058.
Roberts, N., Stevenson, A.C., Davis, B., Cheddadi, R., Brewer, S., Rosen, A., 2004. Holocene climate, environment and cultural change in the circum-Mediterranean region. In: Battarbee, R.W., Gasse, F., Stickley, C. (Eds.), Past Climate Variability Through Europe and Africa (PAGES PEPIII conference volume). Kluwer, Dordrecht, pp. 343–362.
Rodrigo, M.A., Miracle, M.R., Vicente, E., 2001. The meromictic Lake La Cruz (central Spain). Pattern of stratification. Aquatic Sciences 63, 406–416.
Romero-Viana, L., Julià, R., Camacho, A., Vicente, E., Miracle, M.R., 2008. Climate signal in varve thickness: Lake La Cruz (Spain), a case study. Journal of Paleolimnology 40, 703–714.
Sánchez, M., Fernández-Delgado, C., Sánchez-Polaina, F.J., 1992. Nuevos datos acerca de la morfometría y batimetría de la laguna de Zoñar (Aguilar de la Frontera, Córdoba). Oxyura 6, 73–77.
Schulz, M., Stattegger, K., 1997. SPECTRUM: spectral analysis of unevenly spaced paleoclimatic time series. Computers and Geosciences 23, 929–945.
Smoot, J.P., Lowenstein, T.K., 1991. Depositional environments of nonmarine evaporites. In: Melvin, J.L. (Ed.), Evaporites, Petroleum and Mineral Resources. . Development in Sedimentology, 50. Elservier, Amsterdam, pp. 189–347.
Speranza, A., van Geel, B., van der Plicht, J., 2002. Evidence for solar forcing of climate change at ca. 850 cal BC from a Czech peat sequence. Global and Planetary Change 35, 51–65.
Stuvier, M., Braziunas, T.F., Grootes, P.M., Zielinski, G.A., 1997. Is there evidence for solar forcing of climate in GISP2 oxygen isotope record? Quaternary Research 48, 259–266.
Teranes, J.L., McKenzie, J.A., Bernascon, S.M., Lotter, A.F., Sturm, M., 1999a. A study of oxygen isotopic fractionation during bio-induced calcite precipitation in eutrophic Baldeggersee, Switzerland. Geochemica and Cosmochimica 63, 1981–1989.
Teranes, J.L., McKenzie, J.A., Lotter, A.F., Sturm, M., 1999b. Stable isotope response to lake eutrophication: calibration of a high-resolution lacustrine sequence from Baldeggersee, Switzerland. Limnology and Oceanography 44, 320–333.
Theissen, K.M., Dunbar, R.B., Rowe, H.D., Mucciarone, D.A., 2008. Multidecadal- to century-scale arid episodes on the northern Altiplano during the middle Holocene. Palaeogeography, Palaeoclimatology, Palaeoecology 257, 361–376.
Van Geel, B., Buurman, J., Waterbolk, H.T., 1996. Archaeological and paleoecological indications of an abrupt climate change in the Netherlands, and evidences for climatological teleconnections around 2650 BP. Journal of Quaternary Science 11, 451–460.
Van Geel, B., Raspopov, O., Renssen, H., van der Plicht, J., Dergachev, V., Meijer, H., 1999. The role of solar forcing upon climate change. Quaternary Science Reviews 18, 331–338.
Vannière, B., Colombaroli, D., Chapron, E., Leroux, A., Tinner, W., Magny, M., 2008. Climate versus human-driven fire regimes in Mediterranean landscapes: the Holocene record of Lago dell'Accesa (Tuscany, Italy). Quaternary Science Reviews 27, 1181–1196.
Valero-Garcés, B.L., González-Sampériz, P., Navas, A., Machín, J., Mata, P., Delgado-Huertas, A., Bao, R., Moreno, A., Carrión, J.S., Schwalb, A., González-Barrios, A., 2006. Human impact since medieval times and recent ecological restoration in a Mediterranean lake: The Laguna Zoñar, southern Spain. Journal of Paleolimnology 35, 441–465.
Vogt, J., 1968. La decadencia de Roma.Metamorfosis de la cultura antigua. 200–500, Madrid.
Wright, V.P., 1990. Carbonate depositional systems I: marine shallow-water and lacustrine carbonates. In: Tucker, M.E., Wright, V.P. (Eds.), Carbonate Sedimentology. Blackwell Scientific Publication, Oxford.
Zanchetta, G., Drysdale, R.N., Hellstrom, J.C., Fallick, A.E., Isola, I., Gagan, M.K., Pareschi, M.T., 2007. Enhanced rainfall in the Western Mediterranean during deposition of sapropel S1: stalagmite evidence from Corchia cave (Central Italy). Quaternary Science Reviews 26, 279–286.
Zolitschka, B., 2003. Dating based on freshwater-and marine laminated sediments. In: Mackay, A., Battarbee, R., Birks, J., Oldfield, F. (Eds.), Global Change in the Holocene. Oxford University Press, New York.